Hinges-Free and Hinges-Locked Modes of a Deformable Multibody Space Station—A Continuum Analysis

Hari B. Hablani*
Rockwell International, Seal Beach, California

An analytical theory of two classes of vehicle modes for a multibody, deformable space station is presented: 1) hinges-free modes and 2) hinges-locked modes. Both modes are defined for the space station completely free in space; the former modes refer to free hinges, and the latter to locked hinges. Associated eigenvalue problems and orthogonality properties are developed and used to arrive at concise linear motion equations. The conciseness transpires because, with these vehicle modes, the translational and rotational deformations of an inboard body at a hinge have a simple modal expansion. Modal momental coefficients associated with both classes of modes are formulated. They play a pivotal role in discretization of partial differential equations governing the dynamics. The analysis is general: elastic deformation is three dimensional, structures have arbitrary geometry and obey Hooke's law of elasticity, and hinges are universal joints. The modal coefficients and dynamics of the space station are illustrated, and the pitfalls in using hinges-locked vehicle modes to predict hinges-free response are identified. A continuum formulation of dynamics of the space station with a mobile manipulator is also furnished.

I. Introduction

FOR simulating dynamics and control of an inertially stabilized multibody spacecraft, deformations of its elastic components have been variously treated. Generally, it is expressed in terms of appendage modes. To improve fidelity of the simulation, appendage modes of "augmented bodies" have also been suggested.[1] In 1975, Hughes,[2] while dealing with the dynamics of the remote manipulator arm, which consists of several links and is attached to the Orbiter, expressed the deformation of the arm in terms of "fixed-hinge arm mode" (see Sec. 3.1, p. 5, of Ref. 2). These modes are obtained by constraining the Orbiter (the main body) to zero rotation and translation and by constraining the rotation at the hinges of the links of the arm. The hinges are, of course, allowed to translate freely in these modes. Intuitively, these modes are superior to link modes because one fixed-hinge arm mode contains, loosely speaking, one mode of each link plus the dynamic interaction between the links. In 1979, Hughes[3] employed these modes to discretize the dynamics of a chain of flexible bodies. In Ref. 2, Hughes also conceived of a "fixed-hinge spacecraft mode," a vehicle mode, which is defined by locking, as before, all hinges in order to suppress the relative rotation of the articulated bodies, but which allows the entire spacecraft to vibrate freely in space. Hughes expanded on this idea in Ref. 4, in which he defined "external" and "internal" rigid-body (ERB and IRB) modes, where the former are the standard six rigid modes of a free spacecraft and the latter include articulation, ball-in-tube damper, wheel, or any other internal rigid-body motion (see Ref. 4, pp. 7.68-7.88). To facilitate modal analysis of a multibody spacecraft, Hughes[4] then defined the "IRB-constrained mode," which subsumes his earlier[2] "fixed-hinge spacecraft mode," and "IRB-unconstrained mode,"[2] which are defined by keeping hinges as well as spacecraft free in space. However, these ideas have not been pursued in detail in Ref. 4. Because, in this paper, the internal rigid-body motion is articulation motion at hinges, we shall use the alternative name "hinges-locked" instead of "IRB-constrained," and "hinges-free" instead of "IRB-unconstrained" vehicle modes. Hinges-locked vehicle modes are indeed the same as the unconstrained vehicle modes theorized by Hughes[5] for a spacecraft with cantilevered appendages. A distinct characteristic of the hinges-locked and hinges-free modes is that the entire multibody spacecraft is treated as a single elastic body. Interestingly, DISCOS can also treat multibody spacecraft in that manner by expressing the deformation in terms of what Bodley et al.[6] call "geometry modes" in demonstration problems 2 and 4, and "normal modes" in demonstration problem 3. However, Ref. 6 employs Lagrange multipliers and therefore does not offer a minimum number of motion equations for a multibody vehicle. Jones[7] determines system modes for a flexible multibody spacecraft using the classical Craig-Bampton component modal synthesis technique and updates them as the articulated components transgress the linear range around the past nominal orientation. But Ref. 7 does not furnish a mathematical theory of system modes of multibody spacecraft. In the finite-element discipline, there are sophisticated component modal synthesis techniques, such as that of MacNeal,[8] more recent than that of Craig-Bampton. Indeed, using precisely these techniques, the NASTRAN produces numerical values of both hinges-free and hinges-locked vehicle modes of a multibody spacecraft. Nevertheless, the finite-element theory of component modal synthesis (MacNeal[8] and Hintz,[9] for instance), generally illustrated with aircraft and missile structures, seems remotely related to a flexible multibody spacecraft. Consequently, an analytical theory of hinges-free and hinges-locked vehicle modes of a multibody spacecraft based on continuum mechanics is desired. To develop such a theory is the objective of this paper. This theory is sought because it will then establish a clear interpretation of NASTRAN-generated hinges-free and hinges-locked numerical vehicle modes. The vehicle modes are desirable because, for a given number of equations, they offer a higher-fidelity model than the appendage modes do and ease the process of selecting modes for simulation. They do suffer from this oft-quoted limitation: once the components rotate about their hinges beyond the linear range around a nominal orientation, the modes

Presented as Paper 87-0925 at the AIAA Dynamics Specialist Conference, Monterey, California, April 9-10, 1987; received Feb. 19, 1988; revision received Oct. 14, 1988.

*Engineering Specialist, Guidance and Control Group, Satellite and Space Electronics Division. Senior Member AIAA.

must then be replaced by a new set of appropriate vehicle modes; but this seems a little price to pay for the benefits the vehicle modes offer.

The objectives of this paper are accomplished by considering the dynamics of the power tower configuration of the space station, modeled here as comprising two rigid and seven elastic bodies in a simple tree topology. A combination of ordinary and partial differential equations of motion are developed by employing Hamilton's principle. These equations are then subjected to modal analyses, and the associated continuum eigenvalue problems and orthogonality properties of both types of modes are formulated and used to arrive at concise, linear modal equations of motion that are of the same genre as NASTRAN modal equations. Their conciseness stems from subsuming the translational and rotational deformations at hinges in the continuum system modes. Modal momental coefficients that appear in the discretized equations are formulated. A secondary objective of the paper is to present a continuum set of motion equations of the space station with a mobile manipulator.

II. Continuum Formulation of Space Station Dynamics

In the following linear analysis, different subscripts connote different sets of bodies of the Space Station; specifically, note these ranges:

$$p,q = 0,1,2,3,\ldots,8 \qquad \epsilon = 2,3,\ldots,8$$
$$i,j = 1,2,3,\ldots,8 \qquad m,n = 3,\ldots,8 \qquad (1)$$

Besides, a vector pertaining to the body-p is expressed here, unless stated otherwise, in the body-attached frame $\mathcal{F}_p$. The letters $\mathcal{R}$ and $\mathcal{E}$ signify, respectively, rigid and elastic bodies.

An idealized schematic diagram of the proposed space station (ca. 1985, when this analysis began) is shown in Fig. 1. It comprises two rigid bodies ($\mathcal{R}_0$, $\mathcal{R}_1$) and seven elastic bodies ($\mathcal{E}_\epsilon$, $\epsilon = 2,3,\ldots,8$). The rigid body $\mathcal{R}_0$ is a logistic module. It may be docked with the Space Shuttle, and it has both translational and rotational degrees of freedom. The body $\mathcal{R}_1$, on the other hand, is at the intersection of the longitudinal and transverse keels and, being in the middle of the elastic structure $\mathcal{E}_2$, it alters the nature of the vibrational eigenvalue problem in some peculiar way that will be seen in Sec. III. It houses control moment gyros and other appliances to control the attitude of the spacecraft. The elastic structure $\mathcal{E}_2$ is the entire keel structure, including its longitudinal and transverse branches, and $\mathcal{R}_0$ and $\mathcal{R}_1$ are cantilevered to it. The remaining components $\mathcal{E}_m$ are all elastic and hinged to the keel at different locations. These components are module radiators ($\mathcal{E}_3$, $\mathcal{E}_4$), antennas ($\mathcal{E}_5$, $\mathcal{E}_8$), and solar arrays with radiators ($\mathcal{E}_6$, $\mathcal{E}_7$). All hinges are assumed to be universal joints although, after being developed, the equations can be modified readily to model two or one degree-of-freedom hinges. Nominal undeformed location vectors of the cantilever root O_2, $\boldsymbol{L}_0$, of the hinge O_m, $\boldsymbol{L}_{2m}$, and of the mass center $\oplus_i$, $\boldsymbol{r}_{ci}$ are all defined in different frames in Fig. 2. The frames $\mathcal{F}_0$ and $\mathcal{F}_1$ are attached, respectively, to the bodies $\mathcal{R}_0$ and $\mathcal{R}_1$ at their mass centers $\oplus_0$ and $\oplus_1$, whereas the frames $\mathcal{F}_\epsilon$ ($\epsilon = 2,\ldots,8$) are attached to the body $\mathcal{E}_\epsilon$ at the root O_2 for $\epsilon = 2$ and at the hinges O_m for $m = 3,\ldots,8$. A vector expressed in the frame $\mathcal{F}_q$ is transformed to a vector in the frame $\mathcal{F}_p$ by premultiplying it with the transformation matrix $\boldsymbol{R}_{pq}$.

Masses, Inertias, and Displacements

The mass of body-p is denoted m_p; the mass of the entire spacecraft is m. Then, $m = \Sigma m_p$, where the range of summation over p is given by Eq. (1). The first moment of inertia of $\mathcal{E}_m$ with respect to the hinge O_m and that of any body-j relative to the mass center $\oplus_0$ of $\mathcal{R}_0$ are, respectively,

$$\boldsymbol{c}_m = m_m \boldsymbol{r}_{cm} \qquad \boldsymbol{c}_{0j} = m_j \boldsymbol{r}_{c0j} \qquad (2)$$

where $\boldsymbol{r}_{c0j}$ originating from $\oplus_0$ locates the mass center of the jth body in the frame $\mathcal{F}_0$ (Fig. 2):

$$j = 1,2\text{: } \boldsymbol{r}_{c0j} = \boldsymbol{L}_0 + \boldsymbol{R}_{0j}\boldsymbol{r}_{cj}$$
$$j = m\text{: } \boldsymbol{r}_{c0m} = \boldsymbol{L}_0 + \boldsymbol{R}_{02}\boldsymbol{L}_{2m} + \boldsymbol{R}_{0m}\boldsymbol{r}_{cm} \qquad (3)$$

The first moment of inertia $\boldsymbol{c}$ of the entire spacecraft about the mass center $\oplus_0$ will then be

$$\boldsymbol{c} = m\boldsymbol{r}_c = \Sigma \boldsymbol{c}_{0j} \qquad (4)$$

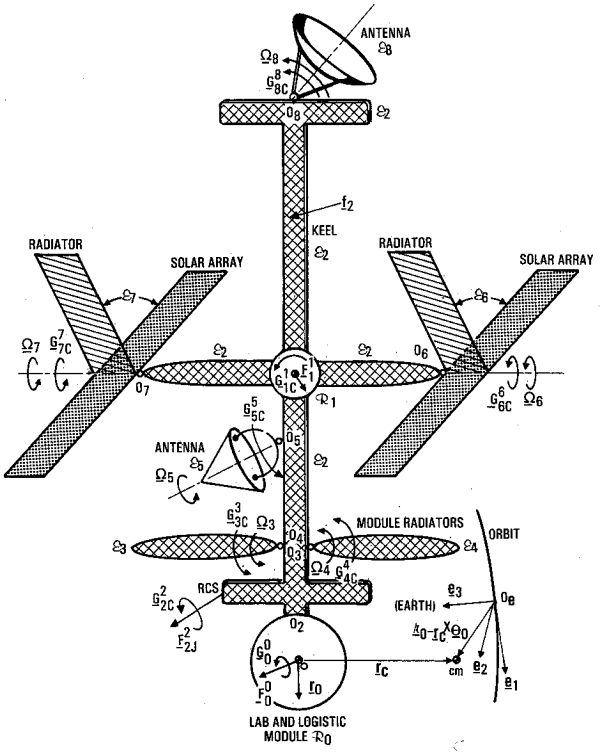

Fig. 1 Schematic model of the space station (power tower configuration).

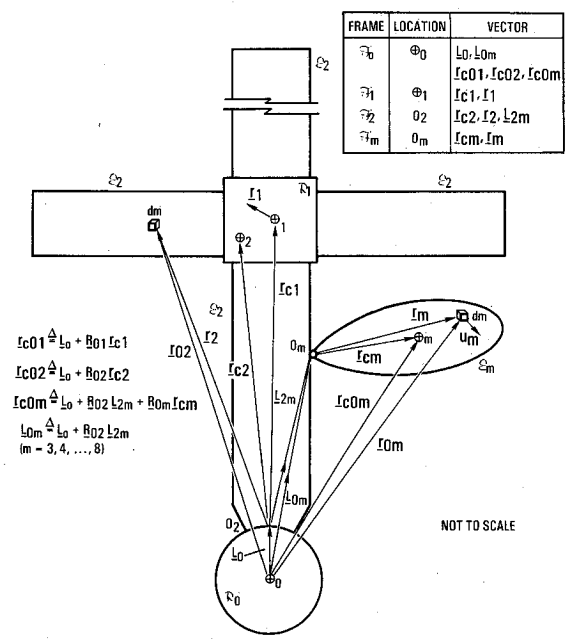

Fig. 2 Location vectors of hinges, mass centers, and elemental masses of component bodies of the space station.

where r_c is the vector from $\oplus_0$ to the vehicle mass center $\oplus$ (Fig. 1). The second moment of inertia of $\Re_0$ and $\Re_1$ about their mass centers $\oplus_0$ and $\oplus_1$ in their local frames are denoted, respectively, I_0 and I_1. On the other hand, J_m is the inertia dyadic of the undeformed body $\mathcal{E}_m$ at the hinge O_m in $\mathcal{F}_m$; J_i^0 is the inertia dyadic of ith body about the mass center $\oplus_0$ in the frame $\mathcal{F}_0$:

$$i=1\colon J_1^0 \triangleq R_{01}I_1R_{10} - m_1 r_{c01}^{\times} r_{c01}^{\times}$$
$$i=\epsilon\colon J_\epsilon^0 \triangleq -\int_\epsilon r_{0\epsilon}^{\times} r_{0\epsilon}^{\times}\, dm \tag{5}$$

where the superscript $\times$ on a vector means the corresponding 3×3 skew-symmetric matrix, the notation $\int_\epsilon$ means integration over the elastic body $\mathcal{E}_\epsilon$, and $r_{0\epsilon}$ is the vector from $\oplus_0$ to an undeformed generic point of $\mathcal{E}_\epsilon$ (Fig. 2):

$$\epsilon=2\colon r_{02} = L_0 + R_{02}r_2$$
$$\epsilon=m\colon r_{0m} = L_0 + R_{02}L_{2m} + R_{0m}r_m \tag{6}$$

and r_ϵ emanates from the origin O_ϵ. Inertial interaction between the mth articulated body and the body $\Re_0$ is represented by a cross-inertia dyadic J_{0m},

$$J_{0m} \triangleq -\int_m r_{0m}^{\times} r_m^{\times}\, dm = R_{0m}J_m - L_{0m}^{\times} R_{0m} c_m^{\times} \tag{7a}$$

where (Fig. 2)

$$L_{0m} = L_0 + R_{02}L_{2m} \tag{7b}$$

Clearly, J_{0m} is not a symmetric dyadic and, in Eq. (7a), it can be postmultiplied only with a vector in the frame $\mathcal{F}_m$. Likewise, the cross-inertia dyadic J_{0m}^T can be postmultiplied only with a vector in the $\mathcal{F}_0$ frame (the superscript T on $[\,\cdot\,]$ signifies the transpose of $[\,\cdot\,]$).

Turning attention to the linear displacements, the local orbital frame $\mathcal{F}_e$ (the unit vector triad e_1,e_2,e_3 in Fig. 1) of the space station is taken to be an inertial frame. Nominally, the origin O_e of the orbital frame coincides with the composite mass center $\oplus$; however, when the spacecraft deviates from its orbital equilibrium, O_e retains the nominal orbital motion while $\oplus$ moves away from O_e by $r_0 - r_c^{\times}\theta_0$, where r_0 and θ_0 are the central, first-order displacement and rotation vectors of $\Re_0$ relative to $\mathcal{F}_e$. The first-order displacement of $\Re_0$ at a field point r_0 is

$$\Re_0\colon w_0 = r_0 - r_0^{\times}\theta_0 \tag{8}$$

The central translational and rotational, perturbational velocities of $\oplus_0$ relative to $\mathcal{F}_e$ are V_0 $(=\dot r_0)$ and Ω_0 $(=\dot\theta_0)$. To determine the displacement of the body $\Re_1$, let $u_2(r_2,t)$ be the deformation at a field point $r_2\epsilon\mathcal{E}_2$, and

$$u_2(0,t) = 0, \qquad \nabla^{\times} u_2(0,t) = 0 \text{ at } r_2 = 0 \tag{9}$$

where ∇ is the del operator. Now, the displacement of the mass center $\oplus_1$ of $\Re_1$, $u_1^*(t)$, and the rotation $\theta_1^*(t)$ of $\Re_1$, both caused solely by u_2, will be

$$u_1^*(t) \triangleq R_{12}u_2(\oplus_1,t) \qquad \theta_1^* \triangleq \tfrac{1}{2}R_{12}[\nabla^{\times} u_x(\oplus_1,t)] \tag{10}$$

Then the deformation-caused angular velocity of $\Re_1$ relative to $\Re_0$ will be $\Omega_1 \triangleq \dot\theta_1^*$. Note that, unlike other articulated bodies, Ω_1 is not a discrete angular velocity. The displacement $w_1(r_1,t)$ of a field point $r_1\epsilon\Re_1$ (Fig. 2) relative to its orbital equilibrium position expressed in the frame $\mathcal{F}_1$ is

$$\Re_1\colon w_1 = R_{10}(r_0 - r_{01}^{\times}\theta_0) + u_1(r_1,t) \tag{11a}$$
$$r_{01} \triangleq L_0 + R_{01}(r_{c1} + r_1) \tag{11b}$$
$$u_1 = u_1^* - r_1^{\times}\theta_1^* \tag{11c}$$

The inertial displacement $w_2(r_2,t)$ of the keel $\mathcal{E}_2$ is

$$\mathcal{E}_2\colon w_2(r_2,t) = R_{20}(r_0 - r_{02}^{\times}\theta_0) + u_2(r_2,t) \tag{12}$$

The deformation u_{2m} and the deformation-caused angular rotation θ_{2m} at each hinge O_m in the frame $\mathcal{F}_2$ are

$$u_{2m}(t) \triangleq u_2(L_{2m},t), \qquad \theta_{2m}(t) \triangleq \tfrac{1}{2}\nabla^{\times} u_2(L_{2m},t)$$
$$(m=3,\ldots 8) \tag{13}$$

Denote the vector of small angles of articulation motion of the body $\mathcal{E}_m$ about the hinge O_m by $\theta_m(\dot\theta_m \triangleq \Omega_m)$, and let the deformation $u_m(r_m,t)$ obey the conditions of zero deformation and zero slope at the root O_m. Then the inertial displacement $w_m(r_m,t)\epsilon\mathcal{E}_m$ is

$$\mathcal{E}_m\colon w_m(r_m,t) = R_{m0}[r_0(t) - r_{0m}^{\times}\theta_0(t)] + R_{m2}u_{2m}(t) - r_m^{\times}(R_{m2}\theta_{2m} + \theta_m) + u_m(r_m,t) \tag{14}$$

To facilitate system modal analysis performed in Sec. III, define

$$U_m(r_m,t) \triangleq R_{m2}u_{2m}(t) - r_m^{\times} R_{m2}\theta_{2m}(t) + u_m(r_m,t)$$
$$(m=3,\ldots,8) \tag{15}$$

which contracts $w_m(r_m,t)$, Eq. (14), to

$$w_m(r_m,t) = R_{m0}[r_0(t) - r_{0m}^{\times}\theta_0(t)] - r_m^{\times}\theta_m(t) + U_m(r_m,t) \tag{16}$$

Clearly, $u_m(r_m,t)$ is local deformation, whereas $U_m(r_m,t)$ is total deformation at $r_m\epsilon\mathcal{E}_m$, treating the entire spacecraft as a single elastic body.

Because the orbital frame $\mathcal{F}_e$ is taken to be inertial, the derivation of inertial velocities of all bodies from Eqs. (8), (11), (12), and (16) and the development of the kinetic energy expression of the space station are straightforward; for details, see Ref. 10. It is reiterated that the variables V_0, Ω_0, Ω_1, Ω_m, and u_ϵ are all first-order infinitesimal quantities; therefore, their products are of second order and thus negligible.

Strain Energy

In this subsection, the comma notation for partial differentiation, and the summation convention for a repeated index, will apply to the indices α and β. The strain energy density function k of a deformable structure is related to stress and strain tensors according to Ref. 11, Eq. (1), p. 127, and Eq. (4), p. 128. Its variation, δk, is found to be

$$\delta k = \sigma_{\alpha\beta}(\delta u_\alpha),_\beta \qquad (\alpha,\beta = x,y,z) \tag{17}$$

where $\sigma_{\alpha\beta}$ is the stress tensor and u_α is the deformation along the α axis. The δK_ϵ variation of the strain energy of the structure $\mathcal{E}_\epsilon$ is related to δk thus:

$$\delta K_\epsilon = \int_\epsilon \delta k\, dv \tag{18}$$

where dv is a volume element of the structure $\mathcal{E}_\epsilon$. Substitute Eq. (17) in (18), and because

$$(\sigma_{\alpha\beta}\delta u_\alpha),_\beta = \sigma_{\alpha\beta}(\delta u_\alpha),_\beta + \delta u_\alpha \sigma_{\alpha\beta},_\beta \tag{19}$$

invoke the Gauss theorem [Ref. 11, Eq. (2), p. 117] to convert the volume integral associated with the term on the left side of Eq. (19) to a surface integral around the boundaries, and obtain

$$\delta K_\epsilon = -\int_\epsilon \sigma_{\alpha\beta},_\beta \delta u_\alpha\, dv + \int_{S_\epsilon} \sigma_{\alpha\beta}\delta u_\alpha \nu_\beta\, dS \tag{20}$$

where $\nu_\beta(\beta = x,y,z)$ are the components of the outward normal ν at the elemental surface area dS of the boundary S_ϵ of the

body $\mathcal{E}_\epsilon$. It is more useful to write the stress tensor $\sigma_{\alpha\beta}$ in terms of displacements and their derivatives. Using the stress-strain relationship for an isotropic elastic material [Ref. 11, Eq. (7), p. 129] and strain-displacement relationship given by Cauchy's infinitesimal strain tensor [Ref. 11, Eq. (6), p. 94], the first term (the volume integral) in Eq. (20) can be rearranged as

$$-\int_\epsilon \sigma_{\alpha\beta,\beta}\delta u_\alpha \, dv = \int_\epsilon (\delta \boldsymbol{u}_\epsilon)^T(\mathcal{L}_\epsilon \boldsymbol{u}_\epsilon)\, dv \tag{21}$$

[the summation convention for the indices α and β does not apply to the right side of Eq. (21)]. The differential operator $\mathcal{L}_\epsilon$ for the isotropic structure $\mathcal{E}_\epsilon$ is [compare the following definition with that in Ref. 11, Eqs. (20) and (19), p. 156, and recall that $\nabla^2 \boldsymbol{u} = \nabla(\nabla\cdot\boldsymbol{u}) - \nabla\times(\nabla\times\boldsymbol{u})$]

$$\mathcal{L}_\epsilon \boldsymbol{u}_\epsilon \triangleq G_\epsilon \nabla\times(\nabla\times\boldsymbol{u}_\epsilon) - (\lambda_\epsilon + 2G_\epsilon)\nabla(\nabla\cdot\boldsymbol{u}_\epsilon) \tag{22}$$

where G_ϵ and λ_ϵ are Lame's constants for the isotropic structure $\mathcal{E}_\epsilon$. Likewise, the boundary integral, the second term in the right side of Eq. (20), can also be written as

$$\int_{S_\epsilon} \sigma_{\alpha\beta}\delta u_\alpha \nu_\beta \, dS = \int_{S_\epsilon} \boldsymbol{\nu}^T \Big[\lambda_\epsilon(\nabla^T \boldsymbol{u}_\epsilon)\mathbf{1} + G_\epsilon\Big\{\boldsymbol{u}_{\epsilon,x} + (\boldsymbol{u}_{\epsilon,x})^T\Big\}\Big]\delta \boldsymbol{u}_\epsilon \, dS \tag{23}$$

where the 3×3 matrix in the square brackets equals symmetric stress tensor, $\mathbf{1}$ is a 3×3 identity matrix, and $\boldsymbol{u}_{\epsilon,x}$ is a 3×3 matrix of partial differentiation of $\boldsymbol{u}_\epsilon$ with respect to the vector $\boldsymbol{x} \triangleq (x_\epsilon, y_\epsilon, x_\epsilon)^T$. For a multibody spacecraft, when the inboard body deforms at the hinges, the motion equations are more compact in terms of the total deformation $\boldsymbol{U}_m(\boldsymbol{r}_m, t)$ defined by Eq. (15) than in terms of the local deformation $\boldsymbol{u}_m(\boldsymbol{r}_m, t)$. For this reason, substitute the variation of Eq. (15) in the right side of Eq. (21) (recall that for $\epsilon = 2$, $\boldsymbol{u}_2 \triangleq \boldsymbol{U}_2$). Next, from the free-body diagram of the mth articulated body, generate two conditions that insure the force and moment balance at the hinge point O_m in the absence of the hinge control torque. The right side of Eq. (21) then transforms to, for $\epsilon = m$,

$$\int_m (\delta \boldsymbol{u}_m)^T(\mathcal{L}_m \boldsymbol{u}_m)\, dv = (\delta \boldsymbol{u}_{2m})^T \boldsymbol{F}_H^{2m} + (\delta\boldsymbol{\theta}_{2m})^T \boldsymbol{G}_H^{2m} + \int_m (\delta \boldsymbol{U}_m)^T(\mathcal{L}_m \boldsymbol{U}_m)\, dv \tag{24}$$

where $\boldsymbol{F}_H^{2m}$ and $\boldsymbol{G}_H^{2m}$ are the unknown constraint forces and torques acting on $\mathcal{E}_m$ and exerted by the body $\mathcal{E}_2$. For a three rotational degree-of-freedom hinge, $\boldsymbol{G}_H^{2m} = \mathbf{0}$; nevertheless, $\boldsymbol{G}_H^{2m}$ is retained here in order to include a hinge with fewer than three degrees of freedom in the analysis. Now, because for all articulated bodies, the deformation $\boldsymbol{u}_m$ satisfies the condition of zero deformation and zero slope at the hinge O_m, the variation $\delta \boldsymbol{u}_m$ in the boundary term Eq. (23) must be zero. Consequently, when we employ Eqs. (20), (21), and (24), the variation in the strain energy of the mth articulated body is found to be

$$\delta K_m = \int_m (\delta \boldsymbol{U}_m)^T(\mathcal{L}_m \boldsymbol{U}_m)\, dv + (\delta \boldsymbol{u}_{2m}^T)\boldsymbol{F}_H^{2m} + (\delta\boldsymbol{\theta}_{2m}^T)\boldsymbol{G}_H^{2m} \qquad (m = 3,\ldots,8) \tag{25}$$

For the keel structure $\mathcal{E}_2$, the boundary S_2 consists of the hinge points O_m ($m = 3,\ldots,8$), collectively called S_2^u, and the interface between $\mathcal{E}_2$ and $\mathcal{R}_1$, denoted by S_2^g. The traction forces and torques $\boldsymbol{F}_H^{m2}$ and $\boldsymbol{G}_H^{m2}$, equal and opposite to $\boldsymbol{F}_H^{2m}$ and $\boldsymbol{G}_H^{2m}$ in Eq. (24), act at the hinge points. Note that the left side of Eq. (23) can also be written involving a traction force $\boldsymbol{T}^\nu$ at the boundary S_2^u [Ref. 11, Eq. (2), p. 63], which then is rearranged in terms of $\boldsymbol{F}_H^{m2}$ and $\boldsymbol{G}_H^{m2}$ to yield

$$\int_{S_2^u} \sigma_{\alpha\beta}\delta u_\alpha \nu_\beta \, dS = \int_{S_2^u} \boldsymbol{T}^\nu \cdot \delta \boldsymbol{u}_2 = \sum_m \Big[(\delta \boldsymbol{u}_{2m}^T)\boldsymbol{F}_H^{m2} + (\delta\boldsymbol{\theta}_{2m}^T)\boldsymbol{G}_H^{m2}\Big] \tag{26}$$

On the other hand, unknown shear forces and bending moments exist at the interface S_2^g. To express these symbolically, note, from Eq. (11b), that

$$@S_2^g: \quad \delta \boldsymbol{u}_2 = \delta \boldsymbol{u}_1 = \delta \boldsymbol{u}_1^* - \boldsymbol{r}_1^\times(S_2^g)\delta\boldsymbol{\theta}_1^* \tag{27}$$

Insert Eq. (27) in the right side of Eq. (23), and define the boundary operators

$$\epsilon = 2: \ \mathcal{B}_u \boldsymbol{u}_2 \triangleq \int_{S_2^g} \Big[\lambda_2(\nabla^T \boldsymbol{u}_2)\mathbf{1} + G_2\Big\{\boldsymbol{u}_{2,x} + (\boldsymbol{u}_{2,x})^T\Big\}\Big]\boldsymbol{\nu}\, dS$$

$$\mathcal{B}_\theta \boldsymbol{u}_2 \triangleq \int_{S_2^g} \boldsymbol{r}_1^\times(S_2^g)\Big[\lambda_2(\nabla^T \boldsymbol{u}_2)\mathbf{1} + G_2\Big\{\boldsymbol{u}_{2,x} + (\boldsymbol{u}_{2,x})^T\Big\}\Big]\boldsymbol{\nu}\, dS \tag{28}$$

where, recall, G_2 is Lame's constant for the elastic body-2. Then, based on Eqs. (20), (21), (23), and (26–28), the variation in the strain energy of the keel structure, δK_2, is obtained:

$$\delta K_2 = -\sum_m \Big\{(\delta \boldsymbol{u}_{2m}^T)\boldsymbol{F}_H^{2m} + (\delta\boldsymbol{\theta}_{2m}^T)\boldsymbol{G}_H^{2m}\Big\} + \int_2 (\delta \boldsymbol{u}_2)^T \mathcal{L}_2 \boldsymbol{u}_2 \, dv + (\mathcal{B}_u \boldsymbol{u}_2)^T \delta \boldsymbol{u}_1^* + (\mathcal{B}_\theta \boldsymbol{u}_2)^T \delta\boldsymbol{\theta}_1^* \tag{29}$$

The variation in the strain energy of the entire vehicle, δK, is derived by adding δK_m ($m = 3,\ldots,8$), Eq. (25), and δK_2, Eq. (29). The nonworking constraint forces and torques at hinges cancel mutually, and we arrive at

$$\delta K = \sum \int_\epsilon (\mathcal{L}_\epsilon \boldsymbol{u}_\epsilon)^T \delta \boldsymbol{U}_\epsilon \, dv + (\mathcal{B}_u \boldsymbol{u}_2)^T \delta \boldsymbol{u}_1^* + (\mathcal{B}_\theta \boldsymbol{u}_2)^T \delta\boldsymbol{\theta}_1^* \tag{30}$$

Surprisingly, we could almost write Eq. (30) by inspection if we treat the space station as one elastic body and use total deformation variable $\boldsymbol{U}_\epsilon$ [note that $\mathcal{L}_\epsilon \boldsymbol{u}_\epsilon = \mathcal{L}_\epsilon \boldsymbol{U}_\epsilon$] because then the unknown constraint forces at hinges do not appear in the analysis. The painstaking and perhaps prima facie abstruse derivation above is nevertheless presented so as to erect a logical scaffolding for Eq. (30).

External and Control Forces and Torques

Let $\boldsymbol{F}_p^p$ and $\boldsymbol{G}_p^p$ be a force and a torque acting, respectively, at and about the mass center $\oplus_p$ of $\mathcal{R}_p$ ($p = 0$ and 1 only). If control moment gyros reside in $\mathcal{R}_1$, the torque exerted by them is included in $\boldsymbol{G}_1^1$. The torque experienced at $\oplus_0$ because of $\boldsymbol{F}_1^1$ and $\boldsymbol{G}_1^1$ will be $\boldsymbol{G}_1^0$, where

$$\boldsymbol{G}_1^0 \triangleq \boldsymbol{R}_{01}\boldsymbol{G}_1^1 + \boldsymbol{r}_{c01}^\times \boldsymbol{R}_{01}\boldsymbol{F}_1^1 \tag{31}$$

Next, let $\boldsymbol{f}_\epsilon(\boldsymbol{r}_\epsilon, t)$ be a distributed force per unit volume acting at $\boldsymbol{r}_\epsilon \epsilon \mathcal{E}_\epsilon$. With the aid of the Dirac delta function and the del operator ∇, $\boldsymbol{f}_\epsilon(\boldsymbol{r}_\epsilon, t)$ can model a point force $\boldsymbol{F}_{\epsilon J}^\epsilon(t)$ at $\boldsymbol{r}_{\epsilon J} \epsilon \mathcal{E}_\epsilon$ produced by jets, a distributed torque $\boldsymbol{g}_\epsilon(\boldsymbol{r}_\epsilon, t)$, or a concentrated torque $\boldsymbol{G}_\epsilon^\epsilon(t)$ at $\boldsymbol{r}_{\epsilon G} \epsilon \mathcal{E}_\epsilon$ exerted by reaction wheels or control moment gyros, for when they all act simultaneously,

$$\boldsymbol{f}_\epsilon(\boldsymbol{r}_\epsilon, t) = \boldsymbol{F}_{\epsilon J}^\epsilon(t)\delta(\boldsymbol{r}_\epsilon - \boldsymbol{r}_{\epsilon J}) + \tfrac{1}{2}\nabla^\times\Big[\boldsymbol{g}_\epsilon(\boldsymbol{r}_\epsilon, t) + \boldsymbol{G}_\epsilon^\epsilon(t)\delta(\boldsymbol{r}_\epsilon - \boldsymbol{r}_{\epsilon G})\Big] \tag{32}$$

where $\delta(\boldsymbol{r}_\epsilon - \boldsymbol{r}_{\epsilon J})$ is a three-dimensional delta function. The total force $\boldsymbol{F}_\epsilon^\epsilon$, the total torque $\boldsymbol{G}_m^m$ about the hinges O_m, and the

torque G_ϵ^0 about $\oplus_0$ arising from f_ϵ are

$$F_\epsilon^\epsilon = \int_\epsilon f_\epsilon(r_\epsilon,t)\,dv, \qquad G_m^m = \int_m r_m^\times f_m\,dv,$$

$$G_\epsilon^0 = \int_\epsilon r_{0\epsilon}^\times R_{0\epsilon} f_\epsilon(r_\epsilon,t)\,dv \tag{33}$$

These external forces and torques are reactionless, unlike the control torque G_{mc}^m acting on $\mathcal{E}_m$ at the hinge O_m. Finally, the total external or control force F_T and torque G_T acting on the space station about the mass center $\oplus_0$ are

$$F_T = \sum R_{0p} F_p^p \qquad G_T = \sum G_p^0 \tag{34}$$

The virtual work performed by the preceding forces and torques is derived in Ref. 10.

Continuum Equations of Motion

If we invoke Hamilton's principle on the variation of kinetic and strain energies and on the virtual work, we obtain the following linear equations of motion of the space station in the neighborhood of the orbital equilibrium:

$$m\dot V_0 - c^\times \dot\Omega_0 - \sum R_{0m} c_m^\times \dot\Omega_m + m_1 R_{01}\ddot u_1^* + \sum \int_\epsilon R_{0\epsilon}\ddot U_\epsilon\,dm = F_T \tag{35a}$$

$$c^\times \dot V_0 + J\dot\Omega_0 + \sum J_{0m}\dot\Omega_m + m_1 r_{c01}^\times R_{01}\ddot u_1^* + R_{01} I_1 \ddot\theta_1^* + \sum \int r_{0\epsilon}^\times R_{0\epsilon}\ddot U_\epsilon\,dm = G_T \tag{35b}$$

$$c_m^\times R_{m0}\dot V_0 + J_{0m}^T\dot\Omega_0 + J_m\dot\Omega_m + \int_m r_m^\times \ddot U_m\,dm = G_{mc}^m + G_m^m \qquad (m = 3,\ldots,8) \tag{35c}$$

$$\left.\begin{aligned} m_1(R_{10}\dot V_0 - R_{10} r_{c01}^\times \dot\Omega_0 + \ddot u_1^*) + R_{12}(\mathcal{B}_u u_2) &= F_1^1 \qquad (35d)\\ I_1(R_{10}\dot\Omega_0 + \ddot\theta_1^*) + R_{12}(\mathcal{B}_\theta u_2) &= G_1^1 \qquad (35e)\end{aligned}\right\} @S_\sigma$$

$$\mathcal{L}_2 u_2 + \sigma_2(R_{20}\dot V_0 - R_{20} r_{02}^\times \dot\Omega_0 + \ddot u_2) = f_2(r_2,t) \tag{35f}$$

$$\mathcal{L}_m u_m + \sigma_m(R_{m0}\dot V_0 - R_{m0} r_{0m}^\times \dot\Omega_0 - r_m^\times \dot\Omega_m + \ddot U_m) = f_m(r_m,t) \qquad (m = 3,\ldots,8) \tag{35g}$$

Equation (35a) governs the translational motion r_0, Eq. (35b) the attitude motion θ_0 of the spacecraft, and Eq. (35c) the angular motion θ_m of the articulated components. The partial differential equations (35f) and (35g) govern the deformational motion of the elastic bodies $\mathcal{E}_\epsilon(\epsilon = 2,\ldots,8)$, and σ_ϵ is their mass density. Although Eqs. (35d) and (35e) are the translational and rotational motion equations of the body $\mathcal{R}_1$, they govern no new discrete variables; instead, they are boundary conditions for Eq. (35f). Other boundary conditions that apply to Eqs. (35f) and (35g) are Eq. (9) and analogous ones for u_m at $r_m = 0$ $(m = 3,\ldots,8)$.

Although the example of the space station is much simpler than an arbitrary multibody deformable spacecraft, Eqs. (35) have all those complications that are present in the latter case: 1) the partial differential equations governing $u_\epsilon(r_\epsilon,t)$ have forcing terms that arise from the spacecraft's overall motion V_0 and Ω_0, from the articulation motion Ω_m and, equally important, from the deformation u_{2m} and the deformation-caused rotation θ_{2m} at the hinge O_m; and 2) the boundary conditions (35d) and (35e) are nonhomogeneous. Just mentioned quantities u_{2m} and θ_{2m} are present in U_m in Eq. (35g). The discrete and deformational variables in Eqs. (35) are linearly coupled; that is, the coupling is of first order. Two system modal analyses are now presented, each of which discretizes the complete set of Eqs. (35) at once.

III. Modal Analyses of Continuum Equations

Discretization by Hinges-Free Vehicle Modes

The space station, like any other spacecraft, has six external rigid modes and, assuming all hinges to be universal joints, three rotational rigid modes for each of the hinged bodies. Additionally, it has (theoretically) an infinite number of elastic modes, labeled $\mu,\nu = 1,\ldots,\infty$. Hence, the following expansion of the discrete variables is complete:

$$\begin{bmatrix} r_0(t)\\ \theta_0(t)\\ \theta_3(t)\\ \cdot\\ \cdot\\ \cdot\\ \theta_8(t)\end{bmatrix} = \begin{bmatrix} R_0(t)\\ \Theta_0(t)\\ \Theta_3(t)\\ \cdot\\ \cdot\\ \cdot\\ \Theta_8(t)\end{bmatrix} + \sum_{\nu=1}^{\infty} \begin{bmatrix} \chi_{0\nu}\\ \phi_{0\nu}\\ \phi_{3\nu}\\ \cdot\\ \cdot\\ \cdot\\ \phi_{8\nu}\end{bmatrix} \eta_\nu(t) \tag{36}$$

where R_0, Θ_0, $\Theta_3,\ldots,\Theta_8$ are "rigid" coordinates, whereas $\eta_\nu(\nu = 1,\ldots,\infty)$ is an elastic modal coordinate. The second column in the right side of Eq. (36) embodies participation of each elastic mode in the discrete motion of the spacecraft. The rigid modes associated with the rigid coordinates are: **1** with $R_0(t)$, $-r_{0p}^\times$ $(p = 0,1,\ldots,8)$ with $\Theta_0(t)$, and $-r_m^\times$ with $\Theta_m(t)$ $(m = 3,\ldots,8)$. A hinges-free vehicle elastic mode is denoted $Z_\nu(r)$. The inertial displacement $w(r,t)$, therefore, of an elemental volume v at $r\epsilon\mathcal{V}$ has this expansion:

$$w(r,t) = R_0(t) - r_{0p}^\times \Theta_0(t) - R_{0m} r_m^\times \Theta_m(t) + \Sigma Z_\nu(r)\eta_\nu(t) \tag{37}$$

Not surprisingly, the system mode $Z_\nu(r)$ consists of the modal coefficients $\chi_{0\nu},\phi_{0\nu},\phi_{m\nu}$ $(m = 3,\ldots,8)$ and the eigenfunction $Z_{i\nu}$ $(i = 1,\ldots,8)$, which are defined over different bodies of the vehicle:

$$Z_\nu(r) \triangleq \chi_{0\nu} - r_{0p}^\times \phi_{0\nu} - R_{0m} r_m^\times \phi_{m\nu} + R_{0i} Z_{i\nu}(r_i) \tag{38}$$

For the rigid body $\mathcal{R}_1$,

$$Z_{1\nu}(r_1) \triangleq \chi_{1\nu} - r_1^\times \phi_{1\nu} \tag{39a}$$

where $\chi_{1\nu}$ and $\phi_{1\nu}$ are νth mode translation of, and rotation about, the mass center $\oplus_1$ of $\mathcal{R}_1$ relative to the body $\mathcal{B}_0$; this implies

$$\chi_{1\nu} \triangleq Z_{2\nu}(\oplus_1), \qquad \phi_{1\nu} = \tfrac{1}{2}\nabla^\times Z_{2\nu}(\oplus_1) \tag{39b}$$

$$u_1^* = \Sigma\chi_{1\nu}\eta_\nu(t), \qquad \theta_1^*(t) = \Sigma\phi_{1\nu}\eta_\nu(t) \tag{39c}$$

For the elastic bodies, $Z_{\epsilon\nu}(r_\epsilon)$ is a deformation field such that the total deformation $U_\epsilon(r_\epsilon,t)$, $r_\epsilon\epsilon\mathcal{E}_\epsilon$, has this expansion:

$$U_\epsilon(r_\epsilon,t) = \Sigma Z_{\epsilon\nu}(r_\epsilon)\eta_\nu(t) \tag{40}$$

Recalling the definition [Eq. (15)] of $U_m(r_m,t)$, the modal expansions of the deformation $u_{2m}(t)$ and the deformation-caused rotation $\theta_{2m}(t)$ of the structure $\mathcal{E}_2$ at the hinge O_m are derived from the expansion of $U_2(r_2,t) \triangleq u_2(r_2,t)$ in Eq. (40):

$$u_{2m}(t) = \sum Z_{2\nu}(O_m)\eta_\nu(t) \qquad \theta_{2m}(t) = \tfrac{1}{2}\sum \nabla^\times Z_{2\nu}(O_m)\eta_\nu(t) \tag{41}$$

It is illuminating to determine the modal expansion of the local deformation $u_m(r_m,t)$ also, knowing the expansions [Eqs. (40)

and (41)] and the relationship [Eq. (15)] between $U_m(r_m,t)$ and $u_m(r_m,t)$; using these formulas, we obtain

$$u_m(r_m,t) = \sum A_{m\nu}(r_m)\eta_\nu(t)$$

$$A_{m\nu}(r_m) \triangleq Z_{m\nu}(r_m) - \left\{Z_{2\nu}(O_m) - r_m^\times \left(\tfrac{1}{2}\nabla^\times Z_{2\nu}(O_m)\right)\right\} \quad (42)$$

where $A_{m\nu}(r_m)$ is that part of the νth hinges-free vehicle mode that describes the deformation of the articulated body $\mathcal{E}_m$ only; at the hinges O_m, $A_{m\nu}(r_m=0)=0$ and $\frac{1}{2}\nabla^\times A_{m\nu}(r_m=0)=0$, so that $A_{m\nu}$ $(\nu=1,\ldots,\infty)$ resembles, but is not identical to the cantilever modes of an articulated body used commonly for discretization of Eqs. (35).

Substituting the modal expansions [Eq. (36)] in the translational motion Eq. (35a), and enforcing the law of linear momentum conservation, there follows the zero linear momentum property of an elastic mode:

$$m\chi_{0\nu} - c^\times\phi_{0\nu} - \sum R_{0m}c_m^\times\phi_{m\nu} + m_1R_{01}\chi_{1\nu} + \sum\int_\epsilon R_{0\epsilon}Z_{\epsilon\nu}(r_\epsilon)\,dm = 0 \qquad (\nu=1,\ldots,\infty) \quad (43)$$

Define the *modal momentum coefficients* $p_{\epsilon\nu}$ associated with the deformation of each articulated body and p_ν for all elastic structures collectively:

$$p_{\epsilon\nu} \triangleq \int_\epsilon Z_{\epsilon\nu}(r_\epsilon)\,dm \qquad p_\nu = m_1R_{01}\chi_{1\nu} + \sum R_{0\epsilon}p_{\epsilon\nu} \quad (44)$$

where the mass of $\mathcal{R}_1$ is included in p_ν. Equation (43) then abbreviates to

$$m\chi_{0\nu} - c^\times\phi_{0\nu} - \sum R_{0m}c_m^\times\phi_{m\nu} + p_\nu = 0 \quad (45)$$

A parallel development starting from Eq. (35b) yields the zero-angular-momentum property of the νth elastic mode:

$$c^\times\chi_{0\nu} + J\phi_{0\nu} + \sum J_{0m}\phi_{m\nu} + h_\nu = 0 \qquad (\nu=1,\ldots,\infty) \quad (46)$$

where the *modal angular momentum coefficient* h_ν is defined as

$$h_\nu \triangleq m_1r_{c01}^\times R_{01}\chi_{1\nu} + R_{01}I_1\phi_{1\nu} + \Sigma h_{\epsilon\nu}^0$$

$$h_{\epsilon\nu}^0 \triangleq \int_\epsilon r_{0\epsilon}^\times R_{0\epsilon}Z_{\epsilon\nu}(r_\epsilon)\,dm \quad (47)$$

The mass and inertia properties of $\mathcal{R}_1$ and its modal participation coefficients $\chi_{1\nu}$ and $\phi_{1\nu}$ are included in the definition of h_ν in Eq. (47). Next, treating the motion of individual articulated bodies $\mathcal{E}_m$ analogously [Eq. (35c)] the law of conservation of the angular momentum of the articulation motion leads to a zero-angular-momentum-like property expressed as

$$c_m^\times R_{m0}\chi_{0\nu} + J_{0m}^T\phi_{0\nu} + J_m\phi_{m\nu} + h_{m\nu} = 0 \qquad (m=3,\ldots,8) \quad (48)$$

where the modal angular momentum coefficient $h_{m\nu}$ for the articulation motion is defined as

$$h_{m\nu} \triangleq \int_m r_m^\times Z_{m\nu}(r_m)\,dm \qquad (m=3,\ldots,8;\ \nu=1,\ldots,\infty) \quad (49)$$

The modal parts $Z_{\epsilon\nu}(r_\epsilon)$ $(\epsilon=2,\ldots,8)$ of a vehicle mode Z_ν are all governed by different eigenvalue problems, each limited to the corresponding elastic structure $\mathcal{E}_\epsilon$. However, because of $\mathcal{R}_1$, $\mathcal{E}_2$ must be considered separately. The vehicle mode Z_ν for $\mathcal{E}_2$ is [from Eq. (38)]

$$Z_\nu(r_2) = \chi_{0\nu} - r_{02}^\times\phi_{0\nu} + R_{02}Z_{2\nu}(r_2) \quad (50)$$

Equation (35f) then leads to the eigenvalue problem

$$\mathcal{L}_2Z_{2\nu}(r_2) = \omega_\nu^2\sigma_2(R_{20}\chi_{0\nu} - R_{20}r_{02}^\times\phi_{0\nu} + Z_{2\nu}) \quad (51)$$

where ω_ν is the frequency of the νth vehicle mode. The associated boundary conditions, obtained form the motion Eq. (35d) and Eq. (35e) owing to $\mathcal{R}_1$ are

$$\mathcal{B}_uZ_{2\nu} = \omega_\nu^2m_1(R_{20}\chi_{0\nu} - R_{20}r_{c01}^\times\phi_{0\nu} + R_{21}\chi_{1\nu}) \quad (52a)$$

$$\mathcal{B}_\theta Z_{2\nu} = \omega_\nu^2R_{21}I_1(R_{10}\phi_{0\nu} + \phi_{1\nu}) \quad (52b)$$

in which the presence of the eigenvalue ω_ν^2 is attributed to the concentrated mass and inertia of $\mathcal{R}_1$ and to the use of vehicle modes. Compared to Eq. (51), the eigenvalue problem derived from the deformation equation of the articulated bodies [Eq. (35g)] is

$$\mathcal{L}_mZ_{m\nu}(r_m) = \omega_\nu^2\sigma_m\left\{R_{m0}\chi_{0\nu} - R_{m0}r_{0m}^\times\phi_{0\nu} - r_m^\times\phi_{m\nu} + Z_{m\nu}(r_m)\right\} \qquad (m=3,\ldots,8) \quad (53)$$

The right sides of the eigenvalue problems [Eqs. (51) and (53)] contain inertial displacement of a field point in the νth mode whereas, in the left sides, the functions $Z_{\epsilon\nu}(r_\epsilon)$ have no discrete motions, only deformational motion. Besides the dynamical boundary conditions (52), the following geometric boundary conditions at the root O_2 and hinges O_m apply:

$$Z_{2\nu}(O_2) = 0, \qquad Z_{2\nu}(O_m) = Z_{m\nu}(O_m)$$

$$\tfrac{1}{2}\nabla^\times Z_{2\nu}(O_2) = 0$$

$$\tfrac{1}{2}\nabla^\times Z_{2\nu}(0_m) = \tfrac{1}{2}\nabla^\times Z_{m\nu}(O_m)$$

$$(\nu=1,\ldots,\infty;\ m=3,\ldots,8) \quad (54)$$

The orthogonality of the vehicle modes $Z_\nu(r)$ with the translational, rotational, and articulational rigid modes $\mathbf{1}$, $-r_{0p}^\times$ $(p=0,1,\ldots,8)$, and $-r_m^\times$, respectively, is expressed as

$$\int_\mathcal{V} Z_\nu\,dm = 0 \quad (55a)$$

$$\int_\mathcal{V} r_{0p}^\times Z_\nu\,dm = 0 \quad (55b)$$

$$\int_m R_{0m}r_m^\times R_{m0}Z_\nu\,dm = 0 \quad (55c)$$

Equations (55) are verified by calling on the mass and inertia properties Equations (2–7), the modal expansions [Eqs. (37) and (40)], and the momentum coefficients [Eqs. (44), (47), and (49)]; this, not surprisingly, yields the momental conditions [Eqs. (45), (46), and (48)], thus proving Eqs. (55). Equipped with these properties, the orthogonality between the elastic modes is found to be

$$\int_\mathcal{V} Z_\mu^TZ_\nu\,dm = m_1\chi_{1\mu}^T(R_{10}\chi_{0\nu} - R_{10}r_{c01}^\times\phi_{0\nu} + \chi_{1\nu}) + \phi_{1\mu}^TI_1(R_{10}\phi_{0\nu} + \phi_{1\nu}) + \sum\int_\epsilon Z_{\epsilon\mu}^TR_{\epsilon0}Z_\nu\,dm$$

$$= p_\mu^T\chi_{0\nu} + h_\mu^T\phi_{0\nu} + m_1\chi_{1\mu}^T\chi_{1\nu} + \phi_{1\mu}^TI_1\phi_{1\nu} + \sum h_{m\mu}^T\phi_{m\nu} + \sum\int_\epsilon Z_{\epsilon\mu}^TZ_{\epsilon\nu}\,dm = \delta_{\mu\nu} \quad (56)$$

where $\delta_{\mu\nu}$ is the Kronecker delta. In the first right-hand side of Eq. (56), the vehicle mode Z_ν is not yet expanded in terms of its components whereas, in the second, it is expanded. The orthogonality between the modes Z_ν and the stiffness op-

erators is obtained using the condition (56), the eigenvalue problems [Eqs. (51) and (53)], and the boundary conditions [Eq. (52)]:

$$\sum\int_\epsilon Z_{\epsilon\mu}^T \mathfrak{L}_\epsilon Z_{\epsilon\nu}\,dv + \omega_\nu^2\Big\{m_1\chi_{1\mu}^T(R_{10}\chi_{0\nu} - R_{10}r_{c01}^\times\phi_{0\nu} + \chi_{1\nu}) + \phi_{1\mu}^T I_1(R_{10}\phi_{0\nu} + \phi_{1\nu})\Big\} = \sum\int_\epsilon Z_{\epsilon\mu}^T \mathfrak{L}_\epsilon Z_{\epsilon\nu}\,dv + \chi_{1\mu}^T R_{12}(\mathfrak{B}_u Z_{2\nu}) + \phi_{1\mu}^T R_{12}(\mathfrak{B}_\theta Z_{2\nu}) = \omega_\nu^2\delta_{\mu\nu} \quad (57)$$

To conserve space, the details of derivation of Eqs. (56) and (57) will not be furnished here.

The set of ordinary and partial differential equations (35) can be discretized now. Substitute the second time derivatives of the expansions of Eqs. (36), (40), and (39c) in Eqs. (35a–35c), and invoke the zero-momental properties [Eqs. (45), (46), and (48)]. This yields the following rigid mode equations corresponding to the vehicle's translation $\boldsymbol{R}_0$, rotation $\boldsymbol{\Theta}_0$, and the articulation angles $\boldsymbol{\Theta}_m$:

$$m\ddot{\boldsymbol{R}}_0 - \boldsymbol{c}^\times\ddot{\boldsymbol{\Theta}}_0 - \Sigma\boldsymbol{R}_{0m}\boldsymbol{c}_m^\times\ddot{\boldsymbol{\Theta}}_m = \boldsymbol{F}_T \quad (58a)$$

$$\boldsymbol{c}^\times\ddot{\boldsymbol{R}}_0 + \boldsymbol{J}\ddot{\boldsymbol{\Theta}}_0 + \Sigma\boldsymbol{J}_{0m}\ddot{\boldsymbol{\Theta}}_m = \boldsymbol{G}_T \quad (58b)$$

$$\boldsymbol{c}_m^\times\boldsymbol{R}_{m0}\ddot{\boldsymbol{R}}_0 + \boldsymbol{J}_{0m}^T\ddot{\boldsymbol{\Theta}}_0 + \boldsymbol{J}_m\ddot{\boldsymbol{\Theta}}_m = \boldsymbol{G}_{mc}^m + \boldsymbol{G}_m^m \quad (m = 3,\ldots,8) \quad (58c)$$

There is no discrete counterpart of the boundary conditions of Eqs. (35d) and (35e). Equations (35f) and (35g) are discretized together. For this purpose, the modal expansions of all variables are inserted in these equations and in the boundary conditions [Eqs. (35d) and (35e)]; Eq. (35f) is then premultiplied with the operation

$$\int_2 Z_{2\mu}^T(\cdot)\,dv$$

Eq. (35g) with

$$\int_m Z_{m\mu}^T(\cdot)\,dv$$

Eq. (35d) with $\chi_{1\mu}^T$, and Eq. (35e) with $\phi_{1\mu}^T$. All of these equations are then added together and simplified, invoking the orthogonality conditions [Eqs. (56) and (57)]. To eliminate the rigid variables $\ddot{\boldsymbol{R}}_0$, $\ddot{\boldsymbol{\Theta}}_0$, and $\ddot{\boldsymbol{\Theta}}_m$ from the discrete equation thus obtained, the transpose of Eqs. (45), (46), and (48) are substituted and Eqs. (58a–58c) are used. We then obtain

$$\ddot{\eta}_\mu + \omega_\mu^2\eta_\mu = \chi_{0\mu}^T\boldsymbol{F}_T + \phi_{0\mu}^T\boldsymbol{G}_T + \chi_{1\mu}^T\boldsymbol{F}_1^1 + \phi_{1\mu}^T\boldsymbol{G}_1^1 + Z_{2\mu}^T(r_{2J})\boldsymbol{F}_{2J} + \sum\phi_{m\mu}^T(\boldsymbol{G}_m^m + \boldsymbol{G}_{mc}^m) + \sum\int_\epsilon Z_{\epsilon\mu}^T\boldsymbol{f}_\epsilon\,dv \quad (\mu = 1,\ldots,\infty) \quad (58d)$$

where $Z_{2\mu}(r_{2J})$ is the modal deflection at the reaction jet locations on the structure $\mathcal{E}_2$; $\boldsymbol{F}_{2J}$ is the jet force. Space limitation forbids giving more details about the derivation of Eq. (58d); however, it is refreshing to see in this equation a systematic inner product of various forces and torques, acting at several locations of the space station, with the corresponding modal translational and rotational coefficients. Equations (58) are the desired discrete equations useful for digital simulation.

Discretizaton by Hinges-Locked Vehicle Modes

The defining property of these modes is that all hinges are locked, although the vehicle as a whole still remains free in space. Mathematically, the constraints are

$$\boldsymbol{\Omega}_m = \boldsymbol{0} \qquad (m = 3,\ldots,8) \quad (59)$$

Incorporating this constraint into the vehicle equations (35a), (35b), and (35g), and deleting Eq. (35c) altogether, these equations, in the absence of external forces and torques, follow:

$$m\dot{\boldsymbol{V}}_0 - \boldsymbol{c}^\times\dot{\boldsymbol{\Omega}}_0 + m_1\boldsymbol{R}_{01}\ddot{\boldsymbol{u}}_1^* + \sum\int_\epsilon \boldsymbol{R}_{0\epsilon}\ddot{\boldsymbol{U}}_\epsilon\,dm = \boldsymbol{0} \quad (60a)$$

$$\boldsymbol{c}^\times\dot{\boldsymbol{V}}_0 + \boldsymbol{J}\dot{\boldsymbol{\Omega}}_0 + m_1\boldsymbol{r}_{c01}^\times\boldsymbol{R}_{01}\ddot{\boldsymbol{u}}_1^* + \boldsymbol{R}_{01}\boldsymbol{I}_1\ddot{\boldsymbol{\theta}}_1^* + \sum\int_\epsilon \boldsymbol{r}_{0\epsilon}^\times\boldsymbol{R}_{0\epsilon}\ddot{\boldsymbol{U}}_\epsilon\,dm = \boldsymbol{0} \quad (60b)$$

$$\left.\begin{aligned} m_1(\boldsymbol{R}_{10}\dot{\boldsymbol{V}}_0 - \boldsymbol{R}_{10}\boldsymbol{r}_{c01}^\times\dot{\boldsymbol{\Omega}}_0 + \ddot{\boldsymbol{u}}_1^*) + \boldsymbol{R}_{12}(\mathfrak{B}_u\boldsymbol{u}_2) &= \boldsymbol{0} \quad (60c)\\ \boldsymbol{I}_1(\boldsymbol{R}_{10}\dot{\boldsymbol{\Omega}}_0 + \ddot{\boldsymbol{\theta}}_1^*) + \boldsymbol{R}_{12}(\mathfrak{B}_\theta\boldsymbol{u}_2) &= \boldsymbol{0} \quad (60d)\end{aligned}\right\} @S_2^\sigma$$

$$\mathfrak{L}_\epsilon\boldsymbol{u}_\epsilon + \sigma_\epsilon(\boldsymbol{R}_{\epsilon0}\dot{\boldsymbol{V}}_0 - \boldsymbol{R}_{\epsilon0}\boldsymbol{r}_{0\epsilon}^\times\dot{\boldsymbol{\Omega}}_0 + \ddot{\boldsymbol{U}}_\epsilon) = \boldsymbol{0} \qquad (\epsilon = 2,\ldots,8) \quad (60e)$$

Equations (60) are similar to those of a spacecraft with cantilevered appendages.[5] For modal analysis, the following expansion is postulated:

$$\begin{aligned} \boldsymbol{r}_0(t) &= \boldsymbol{R}_0(t) + \sum\chi_{0\alpha}^c\eta_\alpha^c(t) & \boldsymbol{u}_1^*(t) &= \sum\chi_{1\alpha}^c\eta_\alpha^c(t)\\ \boldsymbol{\theta}_0(t) &= \boldsymbol{\Theta}_0(t) + \sum\phi_{0\alpha}^c\eta_\alpha^c(t) & \boldsymbol{\theta}_1^*(t) &= \sum\phi_{1\alpha}^c\eta_\alpha^c(t)\\ U_\epsilon(r_\epsilon,t) &= \sum Z_{\epsilon\alpha}^c(r_\epsilon)\eta_\alpha^c(t) \end{aligned} \quad (61)$$

Compare these expansions with those in Eqs. (36), (39c), and (40). The superscript c in Eqs. (61) indicates that these quantities pertain to constrained hinges, whereas the index α ($\alpha = 1,\ldots,\infty$), instead of the previously used (μ,ν), sharpen the difference between hinges-free and hinges-locked modes.

To develop properties of the hinges-locked modes, substitute the expansion (61) first in the translational equation (60a). Employing the law of conservation of linear momentum, we deduce the linear momentum $\boldsymbol{p}_c$ of the vehicle with locked hinges, and the zero-linear-momentum property of a hinges-locked mode:

$$m\dot{\boldsymbol{R}}_0 - \boldsymbol{c}^\times\dot{\boldsymbol{\Theta}}_0 = \boldsymbol{p}_c \quad (62a)$$

$$m\chi_{0\alpha}^c - \boldsymbol{c}^\times\phi_{0\alpha}^c + p_\alpha^c = \boldsymbol{0} \qquad (\alpha = 1,\ldots,\infty) \quad (62b)$$

where the modal momentum coefficient p_α^c is defined as

$$p_\alpha^c = m_1\boldsymbol{R}_{01}\chi_{1\alpha}^c + \sum\boldsymbol{R}_{0\epsilon}\boldsymbol{p}_{\epsilon\alpha}^c p_{\epsilon\alpha}^c = \int_\epsilon Z_{\epsilon\alpha}^c\,dm \quad (63)$$

Compare these with $\boldsymbol{p}_\mu$ and $\boldsymbol{p}_{\epsilon\mu}$ in Eq. (44). Analogously, owing to the law of conservation of angular momentum, substitution of Eq. (61) in Eq. (60b) gives rise to

$$\boldsymbol{c}^\times\dot{\boldsymbol{R}}_0 + \boldsymbol{J}\dot{\boldsymbol{\Theta}}_0 = \boldsymbol{h}_c \quad (64a)$$

$$\boldsymbol{c}^\times\chi_{0\alpha}^c + \boldsymbol{J}\phi_{0\alpha}^c + \boldsymbol{h}_\alpha^c = \boldsymbol{0} \quad (64b)$$

where $\boldsymbol{h}_c$ is the angular momentum of the vehicle with locked hinges, and the modal angular momentum coefficient $\boldsymbol{h}_\alpha^c$ is defined as

$$\boldsymbol{h}_\alpha^c = m_1\boldsymbol{r}_{c01}^\times\boldsymbol{R}_{01}\chi_{1\alpha}^c + \boldsymbol{R}_{01}\boldsymbol{I}_1\phi_{1\alpha}^c + \sum\boldsymbol{h}_{\epsilon\alpha}^{0c}$$

$$\boldsymbol{h}_{\epsilon\alpha}^{0c} = \int_\epsilon \boldsymbol{r}_{0\epsilon}^\times\boldsymbol{R}_{0\epsilon}Z_{\epsilon\alpha}^c\,dm \quad (65)$$

Again, compare Eq. (64b) with Eq. (46), and the definitions of Eq. (65) with Eq. (47). The zero-momentum properties (62b) and (64b) of the hinges-locked vehicle modes are similar to those of the vehicle modes of a spacecraft with cantilevered appendages, a detailed theory of which was set out by Hughes.[5]

To obtain useful dynamic boundary conditions from Eqs. (60c) and (60d), note that, because $\boldsymbol{p}_c$ and $\boldsymbol{h}_c$ in Eqs. (62a) and (64a) are constant and because the associated 6×6 mass matrix is nonsingular, it follows that

$$\ddot{\boldsymbol{R}}_0 = \boldsymbol{0} \qquad \ddot{\boldsymbol{\Theta}}_0 = \boldsymbol{0} \tag{66}$$

The conditions (66), the expansions (61), and the sinusoidal time dependence of the modal coordinate $\eta_\alpha^c(t)$ at the frequency $\omega_{c\alpha}$ lead to these boundary conditions:

$$\mathfrak{B}_u \boldsymbol{Z}_{2\alpha}^c = \omega_{c\alpha}^2 m_1(\boldsymbol{R}_{20}\boldsymbol{\chi}_{0\alpha}^c - \boldsymbol{R}_{20}\boldsymbol{r}_{c01}^{\times}\boldsymbol{\phi}_{0\alpha}^c + \boldsymbol{R}_{21}\boldsymbol{\chi}_{1\alpha}^c) \tag{67a}$$

$$\mathfrak{B}_\theta \boldsymbol{Z}_{2\alpha}^c = \omega_{c\alpha}^2 \boldsymbol{R}_{21}\boldsymbol{I}_1(\boldsymbol{R}_{10}\boldsymbol{\phi}_{0\alpha}^c + \boldsymbol{\phi}_{1\alpha}^c) \tag{67b}$$

which may be compared with their counterparts, Eq. (52). Furthermore, the eigenvalue problem originating from Eq. (60e) owing to the modal expansions [Eqs. (61)] and conditions [Eqs. (66)] is

$$\mathfrak{L}_\epsilon \boldsymbol{Z}_{\epsilon\alpha}^c = \omega_{c\alpha}^2 \sigma_\epsilon(\boldsymbol{R}_{\epsilon 0}\boldsymbol{\chi}_{0\alpha}^c - \boldsymbol{R}_{\epsilon 0}\boldsymbol{r}_{0\epsilon}^{\times}\boldsymbol{\phi}_{0\alpha}^c + \boldsymbol{Z}_{\epsilon\alpha}^c) \qquad (\epsilon = 2,\ldots,8) \tag{68}$$

which is associated with the boundary conditions of Eqs. (67). When the eigenvalue problem (68) is compared with Eq. (53), the absence of the rotation at a hinge in Eq. (68), according to the intrinsic property Eq. (59) of the hinges-locked modes, is evident.

The orthogonality conditions are now determined. The hinges-locked vehicle modes are composed of the modal translation $\boldsymbol{\chi}_{0\alpha}^c$ and rotation $\boldsymbol{\phi}_{0\alpha}^c$ of the entire vehicle, modal translation $\boldsymbol{\chi}_{1\alpha}^c$ and rotation $\boldsymbol{\phi}_{1\alpha}^c$ of $\mathfrak{R}_1$ relative to $\mathfrak{R}_0$, and the modal deformation $\boldsymbol{Z}_{\epsilon\alpha}^c$ $(\epsilon = 2,\ldots,8)$. Analytically, the αth mode is expressed as

$$\boldsymbol{Z}_\alpha^c(\boldsymbol{r}) = \boldsymbol{\chi}_{0\alpha}^c - \boldsymbol{r}_{0p}^{\times}\boldsymbol{\phi}_{0\alpha}^c + \boldsymbol{R}_{0i}\boldsymbol{Z}_{i\alpha}^c(\boldsymbol{r}), \qquad \boldsymbol{Z}_{1\alpha}^c \triangleq \boldsymbol{\chi}_{1\alpha}^c - \boldsymbol{r}_1^{\times}\boldsymbol{\phi}_{1\alpha}^c \tag{69}$$

which, again, may be compared with the hinges-free vehicle mode $\boldsymbol{Z}_\nu(\boldsymbol{r})$ in Eq. (38) and $\boldsymbol{Z}_{\nu 1}(\boldsymbol{r}_1)$ in Eq. (39a). The orthogonality of $\boldsymbol{Z}_\alpha^c$ to the rigid modes $\boldsymbol{1}$ and $-\boldsymbol{r}_{0p}^{\times}$ $(p = 0,1,\ldots,8)$ leads to the conditions

$$\int_{\mathcal{V}} \boldsymbol{Z}_\alpha^c(\boldsymbol{r})\,\mathrm{d}m = \boldsymbol{0} \qquad \int_{\mathcal{V}} \boldsymbol{r}_{0p}^{\times}\boldsymbol{Z}_\alpha^c(\boldsymbol{r})\,\mathrm{d}m = \boldsymbol{0} \tag{70}$$

which are the same as the properties (62b) and (64b). By virtue of Eqs. (70) and (69), the orthogonality of the mode $\boldsymbol{Z}_\alpha^c$ to the mode $\boldsymbol{Z}_\beta^c$ is expressed as follows:

$$\int_{\mathcal{V}} \boldsymbol{Z}_\alpha^{cT}\boldsymbol{Z}_\beta^c\,\mathrm{d}m = m_1\boldsymbol{\chi}_{1\alpha}^{cT}(\boldsymbol{R}_{10}\boldsymbol{\chi}_{0\beta}^c - \boldsymbol{R}_{10}\boldsymbol{r}_{c01}^{\times}\boldsymbol{\phi}_{0\beta}^c + \boldsymbol{\chi}_{1\beta}^c)$$
$$+ \boldsymbol{\phi}_{1\alpha}^{cT}\boldsymbol{I}_1(\boldsymbol{R}_{10}\boldsymbol{\phi}_{0\beta}^c + \boldsymbol{\phi}_{1\beta}^c) + \sum\int_\epsilon \boldsymbol{Z}_{\epsilon\alpha}^{cT}\boldsymbol{R}_{\epsilon 0}\boldsymbol{Z}_\beta^c\,\mathrm{d}m = \delta_{\alpha\beta} \tag{71}$$

Next, the orthogonality of the mode $\boldsymbol{Z}_\alpha^c$ to the stiffness operator $\mathfrak{L}_\epsilon$, Eq. (68), and the boundary operators $\mathfrak{B}_u$ and $\mathfrak{B}_\theta$, Eqs. (67), is found to be

$$\sum\int_\epsilon \boldsymbol{Z}_{\epsilon\alpha}^{cT}\mathfrak{L}_\epsilon\boldsymbol{Z}_{\epsilon\beta}^c\,\mathrm{d}v + \omega_{c\beta}^2\Big\{m_1\boldsymbol{\chi}_{1\alpha}^{cT}(\boldsymbol{R}_{10}\boldsymbol{\chi}_{0\beta}^c - \boldsymbol{R}_{10}\boldsymbol{r}_{c01}^{\times}\boldsymbol{\phi}_{0\beta}^c + \boldsymbol{\chi}_{1\beta}^c)$$
$$+ \boldsymbol{\phi}_{1\alpha}^{cT}\boldsymbol{I}_1(\boldsymbol{R}_{10}\boldsymbol{\phi}_{0\beta}^c + \boldsymbol{\phi}_{1\beta}^c)\Big\} = \omega_{c\alpha}^2\delta_{\alpha\beta} = \sum\int_\epsilon \boldsymbol{Z}_{\epsilon\alpha}^{cT}\mathfrak{L}_\epsilon\boldsymbol{Z}_{\epsilon\beta}^c\,\mathrm{d}v$$
$$+ \boldsymbol{\chi}_{1\alpha}^{cT}\boldsymbol{R}_{12}(\mathfrak{B}_u\boldsymbol{Z}_{2\beta}^c) + \boldsymbol{\phi}_{1\alpha}^{cT}\boldsymbol{R}_{12}(\mathfrak{B}_\theta\boldsymbol{Z}_{2\beta}^c) \tag{72}$$

The stage is now set for discretizing the original Eqs. (35), which include the articulation motion at hinges. Inserting the modal expansion (61) in Eqs. (35a) and (35b) and recalling the zero-momental properties [Eqs. (62b) and (64b)], the vehicle's translation and rotation equations transform to

$$m\ddot{\boldsymbol{R}}_0 - \boldsymbol{c}^{\times}\ddot{\boldsymbol{\Theta}}_0 - \sum\boldsymbol{R}_{0m}\boldsymbol{c}_m^{\times}\ddot{\boldsymbol{\theta}}_m = \boldsymbol{F}_T \tag{73a}$$

$$\boldsymbol{c}^{\times}\ddot{\boldsymbol{R}}_0 + \boldsymbol{J}\ddot{\boldsymbol{\Theta}}_0 + \sum\boldsymbol{J}_{0m}\ddot{\boldsymbol{\theta}}_m = \boldsymbol{G}_T \tag{73b}$$

which resemble Eqs. (58a) and (58b). Because a modal expansion for the articulation angle $\boldsymbol{\theta}_m$ does not exist now, unlike the expansion in Eq. (36) earlier, $\boldsymbol{\theta}_m$ itself appears in Eq. (73a) and (73b). Next, to discretize the rotational motion [Eq. (35c)] at a hinge, define a coefficient $\boldsymbol{h}_{m\alpha}^c$ analogous to Eq. (49):

$$\boldsymbol{h}_{m\alpha}^c = \int_m \boldsymbol{r}_m^{\times}\boldsymbol{Z}_{m\alpha}^c(\boldsymbol{r}_m)\,\mathrm{d}m \qquad (m = 3,\ldots,8;\ \alpha = 1,\ldots,\infty) \tag{74a}$$

and an inertial modal angular momentum coefficient associated with the motion $\boldsymbol{\theta}_m$

$$\boldsymbol{h}_{m\alpha}^{cI} \triangleq \int_m \boldsymbol{r}_m^{\times}(\boldsymbol{R}_{m0}\boldsymbol{\chi}_{0\alpha}^c - \boldsymbol{R}_{m0}\boldsymbol{r}_{0m}^{\times}\boldsymbol{\phi}_{0\alpha}^c + \boldsymbol{Z}_{m\alpha}^c)\,\mathrm{d}m$$
$$= \boldsymbol{c}_m^{\times}\boldsymbol{R}_{m0}\boldsymbol{\chi}_{0\alpha}^c + \boldsymbol{J}_{0m}^T\boldsymbol{\phi}_{0\alpha}^c + \boldsymbol{h}_{m\alpha}^c \tag{74b}$$

Equation (74b) is a counterpart of Eq. (48), except that unlike Eq. (48), Eq. (74b) is not a zero-momentum property. Equation (35c) is now discretized to

$$\boldsymbol{c}_m^{\times}\boldsymbol{R}_{m0}\ddot{\boldsymbol{R}}_0 + \boldsymbol{J}_{0m}^T\ddot{\boldsymbol{\Theta}}_0 + \boldsymbol{J}_m\ddot{\boldsymbol{\theta}}_m + \sum\boldsymbol{h}_{m\alpha}^{cI}\ddot{\eta}_\alpha^c = \boldsymbol{G}_{mc}^m + \boldsymbol{G}_m^m$$
$$(m = 3,\ldots,8) \tag{75}$$

From Eqs. (73) and (75), it is evident that, unlike the hinges-free vehicle modes, the hinges-locked vehicle modes do not decouple $\boldsymbol{R}_0$, $\boldsymbol{\Theta}_0$, and $\boldsymbol{\theta}_m$ $(m = 3,\ldots,8)$ from η_α^c $(\alpha = 1,\ldots,\infty)$. To discretize the partial differential equations (35f) and (35g) in conjunction with the boundary conditions (35d) and (35e), we employ the expansion (61), the properties (62b) and (64b), and the eigenvalue problems (67) and (68). In the process, Eqs. (73) are used to replace $\ddot{\boldsymbol{R}}_0$ and $\ddot{\boldsymbol{\Theta}}_0$ in terms of $\ddot{\boldsymbol{\theta}}_m$, $\boldsymbol{F}_T$, and $\boldsymbol{G}_T$, and the inner product

$$\sum\int_\epsilon \boldsymbol{Z}_{\nu\epsilon}^{cT}(\cdot)\,\mathrm{d}v$$

is performed. These steps yield the modal coordinate equation

$$\sum(\boldsymbol{h}_{m\alpha}^{cI})^T\ddot{\boldsymbol{\theta}}_m + \ddot{\eta}_\alpha^c + \omega_{c\alpha}^2\eta_\alpha^c = \boldsymbol{\chi}_{0\alpha}^{cT}\boldsymbol{F}_T + \boldsymbol{\phi}_{0\alpha}^{cT}\boldsymbol{G}_T + \boldsymbol{\chi}_{1\alpha}^{cT}\boldsymbol{F}_1^1$$
$$+ \boldsymbol{\phi}_{1\alpha}^{cT}\boldsymbol{G}_1^1 + \boldsymbol{Z}_{2\alpha}^{cT}(\boldsymbol{r}_{2J})\boldsymbol{F}_{2J} + \sum\int_\epsilon \boldsymbol{Z}_{\epsilon\alpha}^{cT}\boldsymbol{f}_\epsilon(\boldsymbol{r},t)\,\mathrm{d}v$$
$$(\alpha = 1,\ldots,\infty) \tag{76}$$

Equation (76) does not have, as expected, a term analogous to $\boldsymbol{\phi}_{m\nu}^T(\boldsymbol{G}_m^m + \boldsymbol{G}_{mc}^m)$ of the right side of Eq. (58d). The mass matrix associated with Eqs. (73a), (73b), (75), and (76) is symmetric.

IV. Dynamics of Space Station with a Mobile Manipulator

The space station is outfitted with a mobile manipulator. Our objective now is to modify the continuum equations (35) to incorporate the motion of the manipulator on the deformable keel. Li and Likins[12] have derived the expressions of partial velocities, generalized inertia, and active forces for a cart having mass and moments of inertia and traveling on a curved, deformable track on an inboard or an outboard body of a spacecraft with tree topology. The derivation of final equations of motion, however, for the entire spacecraft is left as an open problem. The problem posed here is simpler: the manipulator is a point mass, and the undeformed track is straight; unlike Ref. 11, though, complete motion equations are furnished here.

Let the instantaneous position of the manipulator on the deformed keel (Fig. 3) be given by a scalar variable $s(t)$, and let $\dot{s}$ be its rectilinear speed along an instantaneous tangent unit vector $\boldsymbol{t}_a$ on the deformed keel $\mathcal{E}_2$. This speed is relative to the instantaneous point of attachment of the manipulator to $\mathcal{E}_2$. In the undeformed position, $s(t)$ equals the location vector $\boldsymbol{r}_{2a}$ emanating from the origin O_2 (Fig. 3). The unit vector triad

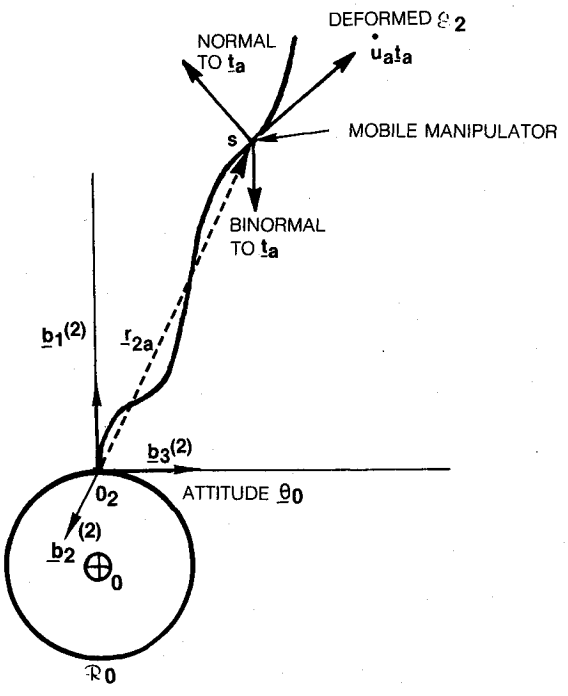

Fig. 3 Mobile manipulator traversing the keel.

$b_1^{(2)}$, $b_2^{(2)}$, $b_3^{(2)}$ associated with the frame $\mathcal{F}_2$ at the origin 0_2 is shown in Fig. 3. In this frame, the unit vector t_a is

$$t_a = \{b_1^{(2)} b_2^{(2)} b_3^{(2)}\}[x_{,s} y_{,s} z_{,s}]^T$$

$$\gamma_{,s} = \frac{d\gamma}{ds} \qquad (\gamma = x,y,z) \tag{77}$$

The derivatives $\gamma_{,s}$ depend on the direction of motion of the manipulator and the deformational rotation θ_{fa} of $\mathcal{E}_2$ at $r_{2a}(t)$. Specifically, if the manipulator is traveling along the $b_1^{(2)}$, $b_2^{(2)}$, or $b_3^{(2)}$ axis, then, in that order,

$$[x_{,s} y_{,s} z_{,s}] = [1 \quad \theta_{fa3} \quad -\theta_{fa2}] \tag{78a}$$

or

$$= [-\theta_{fa3} \quad 1 \quad \theta_{fa1}] \tag{78b}$$

or

$$= [\theta_{fa2} \quad -\theta_{fa1} \quad 1] \tag{78c}$$

where $\theta_{fa} \triangleq [\theta_{fa1} \quad \theta_{fa2} \quad \theta_{fa3}]^T$. Therefore, in general,

$$[x_{,s} y_{,s} z_{,s}]^T = \text{col}\,(1 + \theta_{fa}^{\times}) \tag{79}$$

where col$(\cdot)$ = one of the three columns of $(\cdot)$ depending on the direction of motion of the manipulator. Its inertial velocity $\dot{w}_a$ is

$$\dot{w}_a = \dot{\iota}_0 - r_{02a}^{\times}(t)\dot{\theta}_0 + R_{02}\dot{u}_{2a} + \dot{s}R_{02}\,\text{col}(1 + \theta_a^{\times})$$

$$\theta_a \triangleq \theta_0 + R_{02}\theta_{fa} \tag{80}$$

where θ_a is the vector of the total angle of rotation at the attachment point of the manipulator, $u_{2a}(t) = u_2(r_{2a}, t)$, and $r_{02a}(t) = L_0 + R_{02} r_{2a}(t)$. To determine the inertial acceleration $\ddot{w}_a$ of the manipulator, recognize that

$$\dot{r}_{02a} = \dot{s}\frac{dr_{02a}}{ds} = \dot{s}R_{02}[x_{,s} y_{,s} z_{,s}]^T \tag{81}$$

$$\frac{d}{dt}[x_{,s} y_{,s} z_{,s}] = \dot{s}[x_{,ss} y_{,ss} z_{,ss}] \tag{82}$$

where the second spatial derivatives are obtained by spatial differentiation of Eqs. (78); for instance, corresponding to Eq. (78c)

$$[x_{,ss} y_{,ss} z_{,ss}] = \left[\frac{d\theta_{fa2}}{dz} \quad -\frac{d\theta_{fa1}}{dz} \quad 0\right] \tag{83}$$

The inertial acceleration $\ddot{w}_a$, then, obtained from Eq. (80), is

$$\ddot{w}_a = \ddot{\iota}_0 - r_{02a}^{\times}(t)\ddot{\theta}_0 + R_{02}\ddot{u}_{2a} + \dot{s}^2 R_{02}[x_{,ss} y_{,ss} z_{,ss}]^T$$

$$+ \ddot{s}R_{02}\,\text{col}(1 + \theta_a^{\times}) + 2\dot{s}\,\text{col}(\dot{\theta}_0^{\times}) \tag{84}$$

Let the manipulator be a point mass m_a. The integral of the variation of its kinetic energy T_a is then

$$\int_{t_1}^{t_2} \delta T_a\, dt = -\int_{t_1}^{t_2} m_a \ddot{w}_a^T \delta w_a\, dt \tag{85}$$

where δw_a, from Eq. (80), is

$$\delta w_a = \delta\iota_0 - r_{02a}^{\times}(t)\delta\theta_0 + R_{02}\delta u_{2a} + \delta s R_{02}\,\text{col}(1 + \theta_a^{\times}) \tag{86}$$

In addition, assume that a control force vector $F_a t_a$ acts on the manipulator; this force is taken to be reactionless; that is, it does not produce a reaction force that will act on $\mathcal{E}_2$. The virtual work $\delta\pi$ performed by $F_a t_a$ equals

$$\delta\pi = F_a\{\text{row}[1]\}\{\delta\iota_0 - r_{02a}^{\times}\delta\theta_0 + R_{02}\delta u_{2a}\} + F_a\delta s \tag{87}$$

where row [1] is one of the right-hand sides of Eq. (78) with the rotations θ_{fa} ignored. Incorporating Eqs. (85) and (87) into the original application of Hamilton's principle in Sec. II, the following modified form of Eqs. (35a), (35b), and (35f) and one additional scalar equation for the motion of m_a are obtained:

$$m\ddot{\iota}_0 - c^{\times}\ddot{\theta}_0 - \sum R_{0m} c_m^{\times}\ddot{\theta}_m + m_1 R_{01}\ddot{u}_1^* + \sum\int_{\epsilon} R_{0\epsilon}\ddot{U}_{\epsilon}\, dm$$

$$+ m_a\ddot{w}_a = F_T + F_a\{\text{col}[1]\} \tag{88a}$$

$$c^{\times}\ddot{\iota}_0 + J\ddot{\theta}_0 + \sum J_{0m}\ddot{\theta}_m + m_1 r_{c01}^{\times} R_{01}\ddot{u}_1^* + R_{01} I_1 \ddot{\theta}_1^*$$

$$+ \sum\int_{\epsilon} r_{0\epsilon}^{\times} R_{0\epsilon}\ddot{U}_{\epsilon}\, dm + m_a r_{02a}^{\times}(t)\ddot{w}_a$$

$$= G_T + F_a r_{02a}^{\times}\{\text{col}[1]\} \tag{88b}$$

$$\mathcal{L}_2 u_2 + \sigma_2(R_{20}\ddot{\iota}_0 - R_{20} r_{02}^{\times}\ddot{\theta}_0 + \ddot{u}_2) + m_a R_{20}\ddot{w}_a\delta(r_2 - r_{2a})$$

$$= F_{2J}\delta(r_2 - r_{2J}) + F_a\{\text{col}[1]\}\delta(r_2 - r_{2a}) \tag{88c}$$

$$m_a\{\text{row}[1]\}R_{20}(\ddot{\iota}_0 - r_{02a}^{\times}\ddot{\theta}_0 + R_{02}\ddot{u}_{2a}) + m_a\ddot{s} = F_a \tag{88d}$$

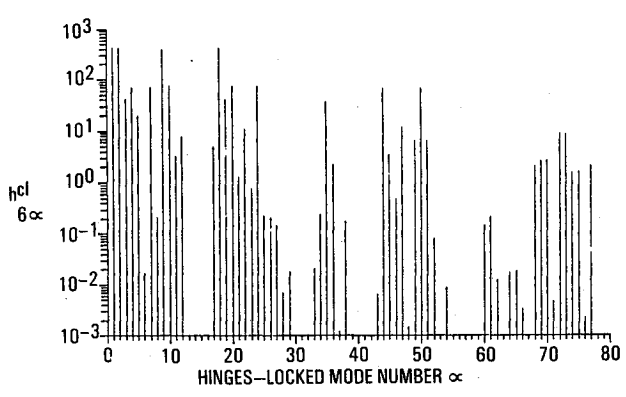

Fig. 4 Modal coupling coefficients $h_{6\alpha}^{cJ}$ ($\alpha = 1, \ldots, 78$) for the solar array $\mathcal{E}_6$ about the y axis.

Table 1 Symmetric 8×8 mass matrix of the space station having only $\mathcal{E}_6$ and $\mathcal{E}_7$ articulated bodies, each with only one axis of relative rotation (MKS units)

0.152847E+06	0.0	0.0	0.0	−0.107233E+07	0.740154E+04	0.0	0.0
0.0	0.152847E+06	0.0	0.107233E+07	0.0	0.425819E+05	0.0	0.0
0.0	0.0	0.152847E+06	−0.740154E+04	−0.425819E+05	0.0	0.0	0.0
0.0	0.107233E+07	−0.740154E+04	0.133607E+09	0.475491E+05	0.799559E+06	0.0	0.0
−0.107233E+07	0.0	−0.425819E+05	0.475491E+05	0.124234E+09	0.522313E+05	0.757040E+06	0.757041E+06
0.740154E+04	0.425819E+05	0.0	0.799559E+06	0.522313E+05	0.143100E+08	0.0	0.0
0.0	0.0	0.0	0.0	0.757040E+06	0.0	0.757041E+06	0.0
0.0	0.0	0.0	0.0	0.757041E+06	0.0	0.0	0.757041E+06

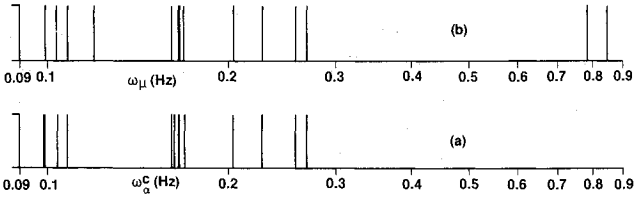

Fig. 5 Natural frequencies of 30 hinges-locked and hinges-free vehicle modes.

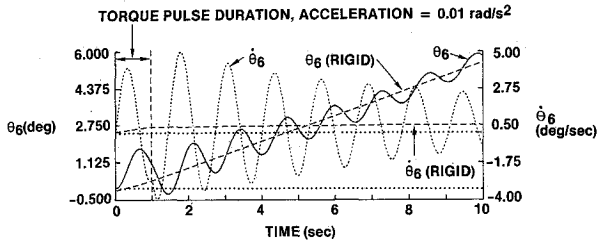

Fig. 6 Response of the solar array $\mathcal{E}_6$ to a torque pulse.

where $\{\text{col}[\mathbf{1}]\} = \{\text{row}[\mathbf{1}]\}^T$. The remaining equations in the set (35) do not change because the manipulator is assumed to travel only on the keel $\mathcal{E}_2$. In the scalar equation of s, Eq. (88d), the Coriolis and the centripetal terms of Eq. (84) do not appear because they are orthogonal to the cart's direction of motion. These terms are nevertheless present in Eqs. (88a–88c).

Discretization of Eqs. (88), along with the unchanged Eqs. (35c–35e) and (35g), is an important matter, but that will not be considered here. It is clear from these equations, though, that now we require the entire mode shape of the structure $\mathcal{E}_2$, unlike the earlier case, in which modal data were needed only at the sensor and actuator locations.

V. Numerical Results and Discussion

Hinges-free discretized equations (58) and hinges-locked discretized equations (73), (75), and (76) are similar to the modal equations that correspond to the NASTRAN-generated numerical data concerning hinges-free and hinges-locked vehicle modes. They will be identical if Eqs. (58a–58c) are subjected to a similarity transformation to arrive at modal rigid modes, and likewise if the 6×6 mass matrix associated with $\boldsymbol{R}_0$ and $\boldsymbol{\Theta}_0$ in Eqs. (73a) and (73b) is orthonormalized by a similarity transformation. In the hinges-free case, selection of elastic modes depends not only on the frequency ω_μ, but also on the modal coefficients $\chi_{0\mu}$, $\phi_{0\mu}$, $\chi_{1\mu}$, $\phi_{1\mu}$, $Z_{2\mu}(r_{2j})$, $\phi_{m\mu}$ ($\mu = 1,\ldots,\infty$; $m = 3,\ldots,8$) in Eq. (58d). Analogously, in the hinges-locked case, the selection depends on the frequency $\omega_{c\alpha}$, the coupling coefficients $h^{cI}_{m\alpha}$, and the coefficients $\chi^c_{0\alpha},\ldots,$ ($\alpha = 1,\ldots,\infty$; $m = 3,\ldots,8$) in Eq. (76). For instance, the scalar coefficients $h^{cI}_{6\alpha}$ ($\alpha = 1,\ldots,78$) for the solar array $\mathcal{E}_6$ about the y axis, which is the axis of once-per-orbit rotation, are shown in Fig. 4 in MKS units. Clearly, from the standpoint of solar array $\mathcal{E}_6$, the hinges-locked vehicle modes $\alpha = 1, 2, 3, 4, 7, 9, 10, 18, 19, 20, 24, 35, 44,\ldots,$ that have larger $h^{cI}_{6\alpha}$ are more important than the remaining modes. Suppose that the space station has only the articulated bodies $\mathcal{E}_6$ and $\mathcal{E}_7$ (solar arrays with radiators) and that these two bodies have only y-rotational degree of freedom. Then, the symmetric 8×8 mass matrix associated with eight discrete degrees of freedom $\boldsymbol{R}_0$, $\boldsymbol{\Theta}_0$, (θ_6, θ_7) [Eqs. (73) and (75)] or (Θ_6, Θ_7) [Eqs. (58a–58c)] is illustrated in Table 1 in MKS units. Here, θ_6 and θ_7 are the angles of rotation of $\mathcal{E}_6$ and $\mathcal{E}_7$ about the y axis relative to the keel, whereas Θ_6 and Θ_7 are their rigid angles of rotation.

Figure 5a illustrates the hinges-locked frequencies $\omega_{c\alpha}$ ($\alpha = 1,\ldots,30$) obtained from NASTRAN, the lowest frequency being close to 0.1 Hz (the ordinate in Fig. 5 has no importance). The hinges-free frequencies ω_μ ($\mu = 1,\ldots$) can be obtained directly from NASTRAN; however, if they are computed from $\omega_{c\alpha}$ ($\alpha = 1,\ldots,30$), those shown in Fig. 5b follow, where ω_{29} (0.78 Hz) and ω_{30} (0.85 Hz) are nearly three times the corresponding ω^c_{29} (0.270 Hz) and ω^c_{30} (0.271 Hz). Experience suggests that the predicted values of ω_{29} and ω_{30} are unreliable. This result is nevertheless shown here because it helps us to understand the simulation results based on hinges-locked modes [Eqs. (73), (75), and (76)] and shown in Fig. 6. Hinges-locked modes are chosen to simulate space station dynamics because, as Ref. 13 demonstrates, for a given number of elastic modes, they furnish a higher-fidelity model than the hinges-free modes do, when a nonzero control torque exists at a hinge. Figure 6 portrays the angle of rotation θ_6 and the rate $\dot{\theta}_6$ of the solar array $\mathcal{E}_6$ subjected to a torque pulse that generates a constant acceleration of 0.01 rad/s^2 for the first second; after that the array is left to swing freely. The variables θ_6 and $\dot{\theta}_6$ pertaining to a rigid solar array are also shown in Fig. 6. The attitude response of the flexible array is seen to be oscillatory (with a damping factor of 0.4%) with a frequency of −0.8 Hz although, surprisingly, the highest hinges-locked vehicle mode frequency present in the simulation is 0.271 Hz. The conclusion emerges that one of the previously mentioned spurious hinges-free modal frequencies, ω_{29} or ω_{30} (although they were never computed to integrate the hinges-locked equations) has manifested itself surreptitiously in the free response of the solar array. Thus, evidently, the simulation program based on hinges-locked modes is not appropriate for studying the free-hinges response, although these modes are more desirable than the hinges-free modes for control design purposes.[13]

VI. Concluding Remarks

The motivation for deriving the preceding two sets of discretized linear equations of motion of a deformable, multibody space station was to be able to rapidly and economically iterate the control systems designs for the entire spacecraft and for the articulated bodies. Strictly speaking, the equations are valid for a three-axis stabilized spacecraft with small motions of all articulated bodies. However, if the spacecraft rotates once per orbit at a small rate (say, 0.06 deg/s, a 100-min orbit), the equations may still be used to design fast control sys-

tems—those that capture target trajectory within, say, 3 min (10.8-deg travel) during which, for instance, the solar arrays tracking the sun would have moved by 5.4 deg from the earlier nominal orientation and during which other articulated bodies may not have transgressed the linear limits. These equations serve other purposes as well. The modal coefficients in the equations indicate the importance of a mode, so that the modes can be selected on the basis of their magnitudes. Besides, a comparison of the two sets of motion equations yields identities between hinges-free and hinges-locked modal parameters.[13] This comparison can be pursued further. Another important extension of this work is to devise hinges-free and hinges-locked vehicle modes for a spacecraft with more complex tree topology than is considered here and with closed loops of flexible bodies. That these equations are formally identical with those arrived at numerically with NASTRAN is immensely fortunate because, as a result, the simulation engineer is disencumbered from solving the preceding complex continuum eigenvalue problems of hinges-free and hinges-locked vehicle modes—NASTRAN having modeled them already via sophisticated finite-element techniques.

Acknowledgment

We sincerely thank Dr. James Keat, Cambridge Research, Cambridge, Massachusetts, for an objective review and constructive criticism of a previous version of this paper.

References

[1]Singh, R. P., Vandervoort, R. J., and Likins, P. W., "Dynamics of Flexible Bodies in Tree Topology—A Computer-Oriented Approach," AIAA Paper 84-1024, 1984, pp. 327-337.

[2]Hughes, P. C., *Motion Equations for a Flexible Articulated Controlled Manipulator Arm, Part II: Comments on Modal Coordinate Alternatives,* Dynacon Enterprises, Dynacon Rept. 75-05-11, Sept. 1975.

[3]Hughes, P. C., "Dynamics of a Chain of Flexible Bodies," *Journal of the Astronautical Sciences,* Vol. XXVII, Oct.-Dec. 1979, pp. 359-380.

[4]Hughes, P. C., "Dynamics of Flexible Spacecraft," lecture notes, Univ. of California, Los Angeles, 1982.

[5]Hughes, P. C., "Modal Identities for Elastic Bodies, With Application to Vehicle Dynamics and Control," *Transactions of the ASME, Journal of Applied Mechanics,* No. 1, Vol. 47, 1980, pp. 177-184.

[6]Bodley, C., Devers, A., Park, A., and Frisch, H., *A Digital Computer Program for Dynamic Interaction and Simulation of Controls and Structures (DISCOS),* NASA TP-1219, May 1978.

[7]Jones, R. E., "Multiflexbody Dynamics for Control Design," *Proceedings of the Workshop on Multibody Simulation,* Vol. I, edited by G. Man and R. L. Laskin, Jet Propulsion Lab., Pasadena, CA, JPL D-5190, April 1988, pp. 354-382.

[8]MacNeal, R. H., "A Hybrid Method of Component Mode Synthesis," *Computers and Structures,* Vol. 1, 1971, pp. 581-601.

[9]Hintz, R. M., "Analytical Methods in Component Mode Synthesis," *AIAA Journal,* Vol. 12, Aug. 1975, pp. 1007-1016.

[10]Hablani, H. B., "Modal Analysis of Dynamics of a Deformable Multibody Spacecraft—The Space Station: a Continuum Approach," *Proceedings of the AIAA Dynamics Specialist Conference,* AIAA, New York, April 1987, pp. 753-768.

[11]Fung, Y. C., *Foundations of Solid Mechanics,* Prentice-Hall, Englewood Cliffs, NJ, 1965.

[12]Li, D. and Likins, P. W., "Dynamics of a Multibody System With Relative Translation on Curved, Flexible Tracks," *Journal of Guidance, Control, and Dynamics,* Vol. 10, May-June 1987, pp. 299-306.

[13]Hablani, H. B., "Modal Identities for Multibody Elastic Spacecraft—An Aid to Selecting Modes for Simulation," AIAA Paper 89-0544, Jan. 1989.